Monatshefte für Chemie - Chemical Monthly (2020) 151:1549–1555
https://doi.org/10.1007/s00706-020-02688-1

ORIGINAL PAPER

Oxidation of toluene to benzoic acid via VOTPP catalyst synthesized with an improved method

Jiaojiao Jia[1,2] · Xi Chen[1,2] · Lijun Zhai[3] · Yulan Niu[2]

Received: 6 February 2020 / Accepted: 14 September 2020 / Published online: 14 October 2020

Abstract

In this paper, two-step method was used to synthesize 5,10,15,20-tetraphenyl-21*H*,23*H*-porphine vanadium(IV) oxide (VOTPP) and toluene catalytic oxidation was explored. The result showed that this catalyst led to benzoic acid as the main product and successfully simulated the reaction of toluene oxidation with the catalytic center of P-450 enzyme. Through testing the reaction conditions including used catalyst amount, temperature, pressure, and reaction time, the optimum reaction conditions were: 0.3 g VOTPP in 100 cm^3 of toluene, 145 °C, 0.8 MPa, and 4 h. The conversion of toluene was 23.0% and the selectivity of benzoic acid could reach 86.0%. Its benefits lie in no solvent, mild reaction conditions, and no toxic acidic waste, making toluene oxidation a green process.

Graphic abstract

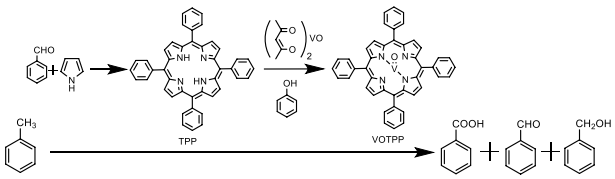

Keywords Toluene · Oxidation · Benzoic acid · VOTPP

Introduction

Benzoic acid, as an important raw material, is widely used in medicine, preservatives, inhibitors, dyestuffs, plasticizers, antirust, etc. [1]. In industry, it is mainly produced from the homogeneous processes, such as benzyl chloride hydrolysis, phthalic anhydride decarboxylation, and toluene oxidation [2]. However, benzyl chloride hydrolysis leads to chlorides in the product, which restricts its use in the field of food preservatives and pharmaceuticals. The final product with the phthalic anhydride decarboxylation is difficult to refine and the cost is high, so that it is only applied in medicine and other industries in small batches. Therefore, toluene oxidation has been regarded as a promising regular method for the commercial benzoic acid production, which has been achieved in acetic acid solution and soluble bromide salt with cobalt or manganese salt as catalysts by heating methylbenzene to 250 °C under high pressure [3]. However, the harsh reaction conditions lead to excessive energy consumption. Most importantly, expensive titanium clad equipment is needed to resist the corrosion of the metal/bromine/acetic acid mixture in the reaction [4, 5].

The research has found that methylbenzene is converted to benzoic acid by the use of acetonitrile solvent with the Nb and NbCo-MCM-41 catalysts in acetonitrile solvent, which can noticeably solve the problem of the acidic waste [6]. By comparing different reaction solvents like acetone, methyl

✉ Yulan Niu
jiao15835130692@163.com

[1] School of Chemical Engineering and Technology, North University of China, Tai Yuan 030051, P. R. China

[2] Institute of Interface Chemistry and Engineering, Taiyuan Institute of Technology, Tai Yuan 030008, P. R. China

[3] 1331 Clean and Renewable Energy Engineering Research Center of Shanxi Province, Taiyuan Institute of Technology, Tai Yuan 030008, P. R. China

alcohol, and acetonitrile, it was found that the environment with acetone could promote the toluene conversion [7]. However, toluene conversion rates are low in these systems, and solvent recovery is also difficult. The heterogeneous catalytic process in toluene oxidation can not only promote toluene conversion rate, but also avoid some operations like solvent recovery.

For example, the toluene catalytic air oxidation with chitosan-supported Co(II)TPP was effectively finished in the absence of reductants and solvents under a relatively mild condition [8]. Bastock efficiently oxidized toluene to benzoic acid within 22 h without solvent [9]. Grapheme-hemin hybrid materials could be used as an efficient catalyst to oxidize toluene, and the benzoic acid selectivity was 85% at the time of 30 h in the absence of solvent [10]. However, it is very difficult to realize industrial production because of the large amount of catalyst, low efficiency, and high cost.

Vanadium plays an important role in the process of toluene oxidation [11–14]. Some study has shown that the catalytic effect of the catalysts on toluene was related to the concentration and distribution of the active sites on vanadium-based catalysts. In these studies, V^{4+} cations were assumed to be the sites for the formation of electrophilic oxygen species participating in deep oxidation [15]. Many studies have shown that metalloporphyrins such as cobalt porphyrin, zinc porphyrin, manganese porphyrin, iron porphyrin, etc. perform a high activity in the oxidation of inert carbon–hydrogen bond of hydrocarbons [16–19]. At present, it has not been found that vanadyl porphyrin is applied to toluene oxidation.

In this paper, the two-step method is adopted to synthesize the VO(IV)TPP catalyst applied to toluene efficient selective oxidation to benzoic acid. Compared with the heterogeneous catalyst, the contact between the substrate and the catalyst is increased, the amount of catalyst is greatly reduced, the reaction time is shortened, no toxic acidic waste is produced, and the process of solvent recovery is eliminated.

Results and discussion

Characterization of TPP and VOTPP

It is seen from Table 1 that TPP and VOTPP are red–purple and pink–purple, respectively, which is consistent with the literature; and the measured contents of chemical composition are also in good agreement with the theoretical results [20, 21].

The UV–Vis spectra of TPP and VOTPP in CH_2Cl_2 solution are shown in Fig. 1. The Soret band strong absorption peak and the Q-band weak absorption peaks are the characteristic peaks of porphyrin [22–25]. Compared with TPP in the region of 300–700 nm, the Soret band shows a red shift of 6 nm to 423 nm after synthesize VOTPP, and the number of the Q-band absorption peaks is reduced [26, 27]. The red shift of the Soret band is related to changes in the TPP plane due to the coordination of N in the pyrrole ring to vanadium. As a result, the metallization of TPP results in the increased molecular symmetry, the closer energy level, the electrons to be more susceptible to excitation, and the higher absorption wavelength. Meanwhile, the increase in molecular symmetry can decrease the splitting of the molecular orbit and the degeneracy is enhanced, which is shown by a decrease in the number of Q-band absorption peaks. The red shift of Soret band and the decrease in the number of Q-band absorption peaks indicate the formation of metalloporphyrins.

The FT-IR spectra of TPP and VOTPP are shown in Fig. 2. The N–H stretching and bending vibration absorption peaks of the TPP pyrrole ring are at 3312 and 964 cm^{-1}, respectively; those peaks at 1596, 1473, and 1441 cm^{-1} are attributed to the vibration absorption of benzene and pyrrole rings; and those peaks at 798 and 699 cm^{-1}, respectively, are attributed to the C–H out-of-plane bending vibration of the benzene ring [26, 28]. Compared with TPP, the characteristic peaks of VOTPP at 3312 and 964 cm^{-1} disappear

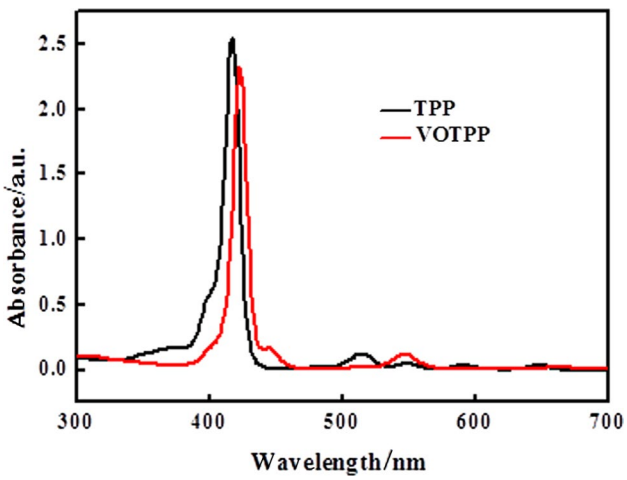

Fig. 1 UV–Vis spectra of TPP and VOTPP in CH_2Cl_2 solution at room temperature

Table 1 Compositions and colors of TPP and VOTPP

Compounds	Compositions	Colors	Exp. (Theor.) /%		
			C	H	N
TPP	$C_{44}H_{30}N_4$	Red–purple	85.3 (85.89)	4.96 (4.88)	9.34 (9.11)
VOTPP	$C_{44}H_{28}N_4VO$	Pink–purple	77.27 (77)	4.23 (4.12)	8.35 (8.24)

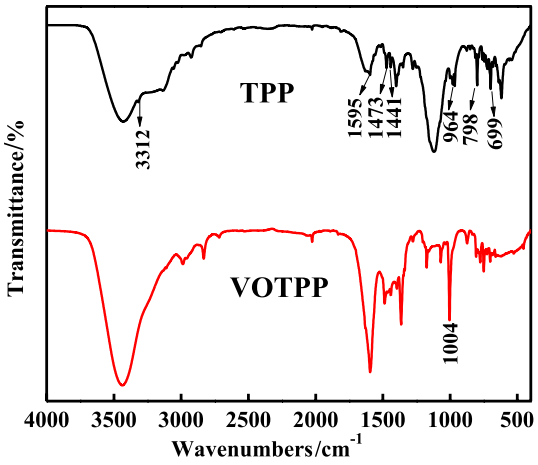

Fig. 2 FT-IR spectra of TPP and VOTPP

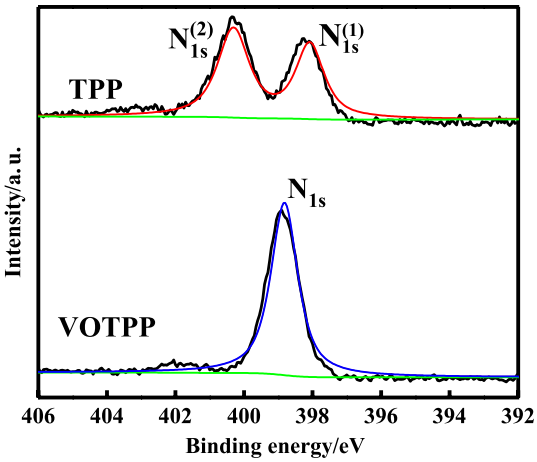

Fig. 4 The binding energies of N_{1s} in TPP and VOTPP

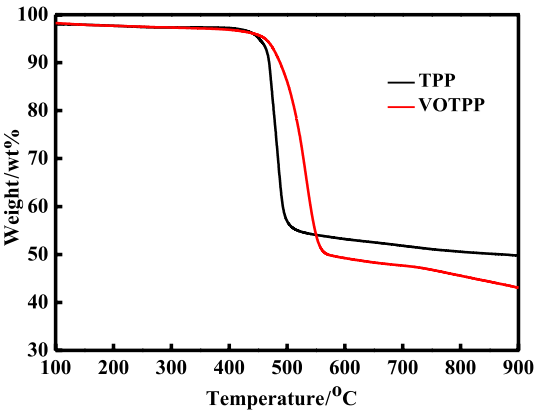

Fig. 3 Weight loss curves of TPP and VOTPP

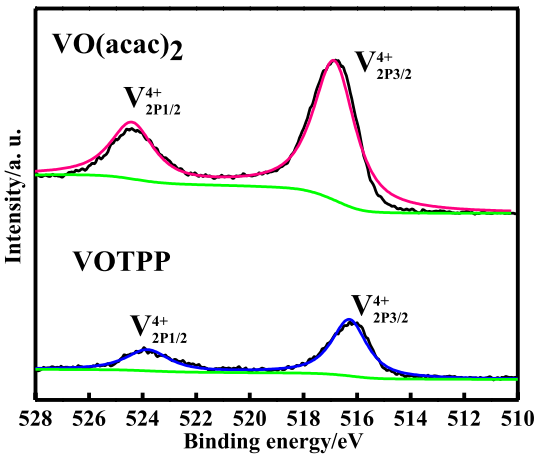

Fig. 5 The binding energies of $V^{4+}{}_{2p}$ in VOTPP and $VO(acac)_2$

and a new strong peak is formed at 1004 cm^{-1} due to the stretching/bending vibration from the combination of VO^{2+} and porphyrin. These observations are in good agreement with the Tsutomu et al.'s results [21, 27], which can be used to estimate the coordination of porphyrin ligands with metal ions.

The TG results of TPP and VOTPP are shown in Fig. 3. It is shown that porphyrin and metalloporphyrin have high thermodynamic stability [29]. The decomposition temperature of VOTPP (450 °C) is higher than that of TPP (420 °C), because the coordination of VO^{2+} with the porphyrin ring reduces the molecular rigidity and intra-ring tension. The presence of oxygen atoms in VO^{2+} allows better coordination of tetravalent vanadium with the porphyrin ring, so the stability of VOTPP is higher than that of TPP.

The N_{1s} peaks of TPP and VOTPP in XPS are shown in Fig. 4. The two N_{1s} peaks of TPP are 397.89 eV ($N_{1s}{}^{(1)}$) and 400.11($N_{1s}{}^{(2)}$), and the peak area ratio is 1:1. They belong to two chemically different N. They are two N($N_{1s}{}^{(1)}$) without H on the pyrrole ring and two N($N_{1s}{}^{(2)}$) with H on the pyrrole ring. From the N_{1s} peaks of TPP and VOTPP in XPS, it is known that there is only one N_{1s} peak, there is only one chemically N, and a binding energy of 398.88 eV [30]. This suggests that the two H on the pyrrole ring of TPP center disappear and are replaced by VO^{2+} to form the complex, which makes the four N atoms chemically identical.

The $V^{4+}{}_{2p}$ peaks of VOTPP and $VO(acac)_2$ in XPS are shown in Fig. 5. From the spectrum of $VO(acac)_2$, the peaks of $V^{4+}{}_{2p1/2}$ and $V^{4+}{}_{2p3/2}$ are at 524.22 eV and 516.57 eV, while after forming the complex, their peaks are at 523.89 eV and 516.33 eV, respectively. Compared with the decrease of the binding energy before coordination, this is due to the electrostatic repulsion that causes the decrease in the electron cloud density in $V^{4+}{}_{2p}$ and, consequently, the decrease in the binding energy.

The O_{1s} peaks of VOTPP and $VO(acac)_2$ in XPS are shown in Fig. 6. From the XPS of $VO(acac)_2$, the O_{1s} peak

is at 531.87 eV, while after forming VOTPP, the binding energy is 532.46 eV, which increased compared with that before the coordination. This is because the additional coordination of the oxygen in VOTPP with porphyrin ring causes the pentacoordinate complex, leading to the increase in O_{1s}-binding energy [29].

The synthesized TPP and VOTPP were analyzed by ^{1}H NMR ($CDCl_3$). The ^{1}H NMR data of TPP mainly showed in −2.78 (s, 2H, N–H), 7.74–7.8 (m, 12H, *m*- and *p*-aryl H), 8.21–8.23 (m, 8H; *o*-aryl H), and 8.85 (s, 8H, β-pyrrole-H). By comparing the ^{1}H NMR spectra of TPP and VOTPP, it has been found that the chemical shift of the H proton in the pyrrole ring in the porphyrin is at −2.78 ppm, while, in the metalloporphyrin, the peak disappears, indicating the formation of a vanadium oxyporphyrin [31, 32].

Catalytic performance of VOTPP for toluene oxidation with O_2

Figure 7 shows the effect of the amount of catalysts on toluene oxidation. It is evident that the conversion of toluene and selectivity of benzoic acid increase with the amount of catalysts. Specifically, the conversion of toluene and the selectivity of benzoic acid and benzaldehyde are low at 0.1 g of VOTPP, but are increased to 22.7%, 85.8%, and 11.9%, respectively, with the increase of the catalyst amount to 0.3 g. However, as the catalyst amount is further increased to 0.5 g, the conversion of toluene is decreased to 21.9%, and the selectivity of benzoic acid and benzaldehyde remains largely unchanged. Notably, the selectivity of benzyl alcohol is still low (1.06–2.01%), which is mainly due to the higher reactivity of benzyl alcohol. Thus, the optimum amount of catalyst is determined to be 0.3 g from an economic perspective. Further batch tests would be performed at this amount.

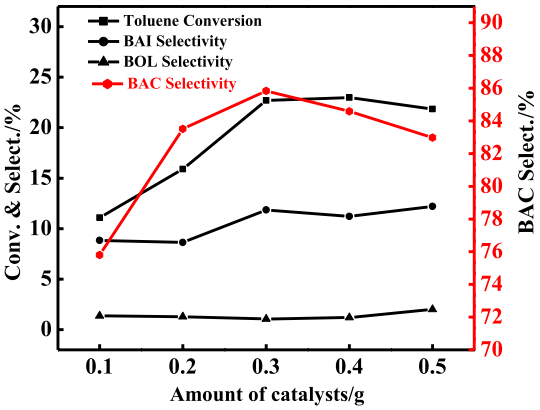

Fig. 7 The effect of the amount of catalyst on toluene oxidation

Toluene conversion and selectivity are related to the amount of the catalyst. Catalyst activity reaches a maximum at 0.3 g of the catalyst in 100 cm^3 of toluene. The mechanism of alkane oxidation catalyzed by metalloporphyrin is similar to that of cytochrome P-450 enzyme-free radical reaction. A too large amount of the catalyst would increase the contact between the active intermediate and the catalyst during the reaction, causing deactivation of a large amount of catalyst and a decrease in reaction activity [33].

Figure 8 shows the effect of reaction temperature on the conversion and selectivity of toluene oxidation with 0.3 g of VOTPP as the catalyst in the presence of oxygen. Increasing temperature is beneficial to the increase in toluene conversion and benzoic acid selectivity. Toluene conversion is 21.6% and benzoic acid selectivity is 85.5% at 145 °C. As the temperature is increased to 165 °C, benzoic acid selectivity is slightly increased to 87.7%, but benzaldehyde selectivity decreases, because increasing temperature contributes to the formation of reactive intermediates. Benzaldehyde conversion to benzoic acid increases, leading to a decrease in benzaldehyde

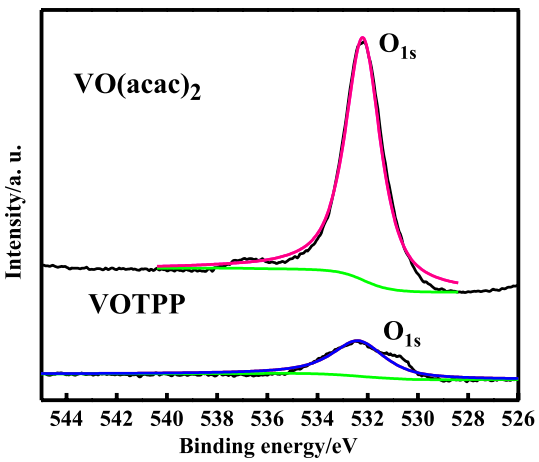

Fig. 6 The binding energies of O_{1s} in VOTPP and $VO(acac)_2$

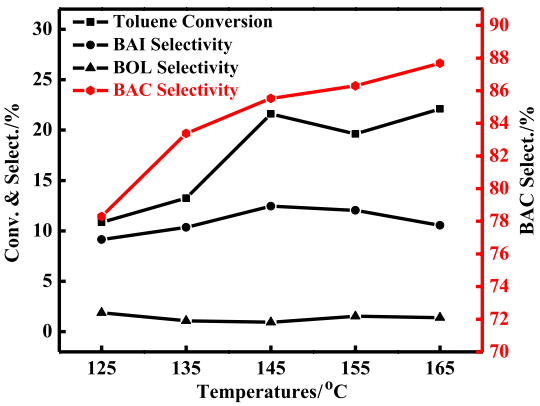

Fig. 8 The effect of reaction temperature on toluene oxidation

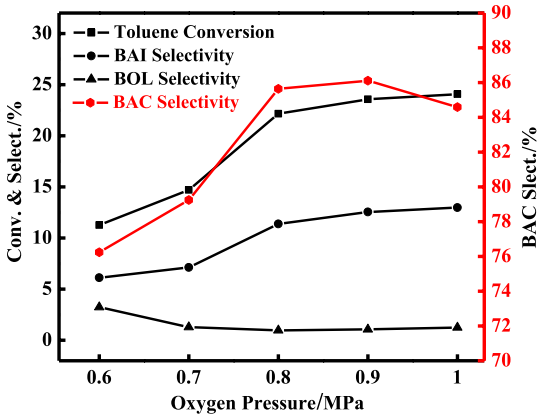

Fig. 9 The effect of reaction pressure on toluene oxidation

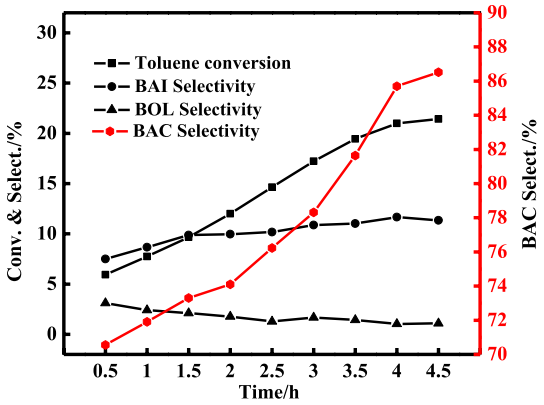

Fig. 10 The effects of reaction time on toluene oxidation

selectivity. Considering all together, the optimal reaction temperature is determined to be 145 °C.

Figure 9 shows the effect of reaction pressure on the oxidation of toluene. Both conversion and selectivity are higher at a pressure of 0.8 MPa, and the oxygen content of the reaction system is low at low pressure. Increasing the pressure will increase the oxygen content and, thus, the reaction activity. However, as the pressure is increased above 0.8 MPa, the toluene conversion rate decreases slightly, which may be related to the saturation concentration of oxygen in the reaction solution. Further batch tests would be performed at 0.8 MPa.

Figure 10 shows the effects of reaction time on toluene oxidation activity. Toluene conversion gradually increases over time and reaches a higher value of 21% at 4 h. Benzoic acid selectivity is more obvious than that of benzaldehyde. Excessive reaction time will lead to excessive oxidation of benzaldehyde to generate more benzoic acid, which will reduce benzaldehyde reactivity. Considering all together, the optimal reaction time is determined to be 4 h.

Conclusions

The catalyst (VOTPP) is prepared by the two-step improved method. It is used to catalyze toluene oxidation under the mild reaction conditions. The results show that the catalyst exhibits an excellent performance when benzoic acid is the main product. The optimum reaction conditions of VOTPP catalysis in toluene oxidation are gained through a series of factor experiments. The optimum reaction conditions are: 0.3 g of the catalyst in 100 cm^3 of toluene, reaction temperature of 145 °C, pressure of 0.8 MPa, and reaction time of 4 h. And toluene conversion is 23.0% and benzoic acid selectivity is 86.0%. Moreover, in this experiment, toluene oxidation under lower pressures and temperature has a remarkable reduction in energy consumption, which shows a better performance. No toxic waste is generated, which makes toluene oxidation more environmentally friendly.

Experimental

o-Xylene, pyrrole, benzaldehyde, salicylic acid, phenol, vanadium(IV) oxyacetylacetonate, and toluene were purchased from Sinopharm Chemical Reagent Co., Ltd. (China). All commercial chemicals were used without further purification.

UV–Vis diffuse reflectance spectroscopy (DRS) was performed (300–700 nm) on a PERSEE TU-1900 spectrophotometer using CH_2Cl_2 as the solvent. The Fourier transform infrared (FT-IR) spectra of samples were recorded on a Perkin Elmer Spectrum 100 spectrometer in the range 400–4000 cm^{-1} using spectral-grade KBr. Thermogravimetric analyses (TGA) of samples (10 mg) were conducted on a TGA4000 (Perkin Elmer) thermogravimetric analyzer in N_2 over the temperature range 20–900 °C at a heating rate of 10 °C /min. Elemental analyses (C, H, and N) were performed with a vario EL cube elementar. ESCALAB 250 Xi XPS spectrometer (Thermo Fisher Scientific) was used with 1486.6 eV Kα Al X-ray source. All ^{1}H NMR measurements were performed using Bruker AVANCE 400 MHz spectrometers in $CDCl_3$.

Gas chromatography (GC) was performed on a GC9790 gas chromatography equipped with a flame ionization detector. The remaining toluene, benzaldehyde, and benzyl alcohol were analyzed in a PEG-20 M column (0.32 mm × 30 m, φ 0.5 μm), where the injection volume of the test solution was 2 mm^3, and the temperature of the detector and inlet was 200 °C. The solution of toluene was diluted with acetone to a certain concentration at an oven temperature of 100 °C. The contents of benzaldehyde

Scheme 1

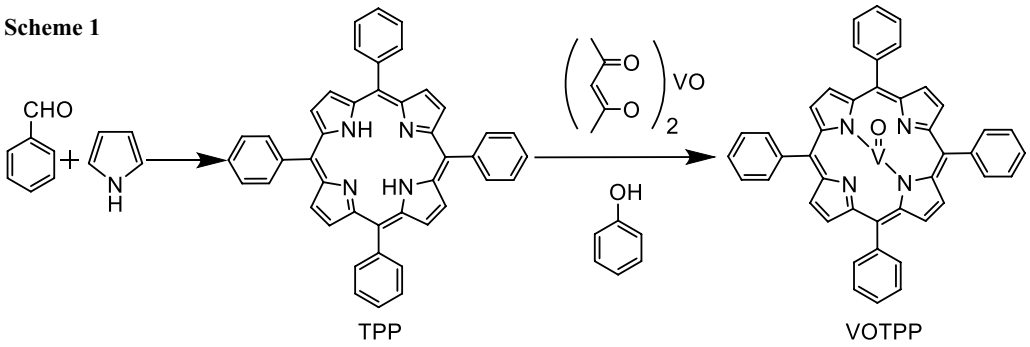

Scheme 2

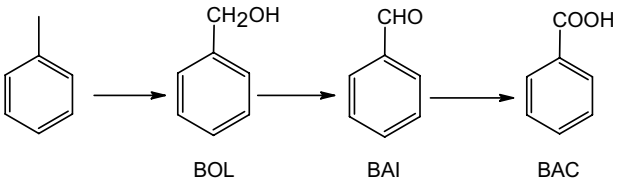

and benzyl alcohol in the reaction solution were directly measured at an oven temperature of 180 °C. The content of benzoic acid was analyzed in a C18 column using Thermo Fisher high-performance liquid chromatography (HPLC). A mixture of 30%(v) formic acid and 70%(v) methanol was used as the mobile phase at a flow rate of 0.2 cm^3/min. The conversion was calculated using Eq. (1):

$$\%\ \text{conversion} = \frac{\text{mass of toluene reduced}/M_{\text{toluene}}}{\text{mass of toluene charged}/M_{\text{toluene}}} \times 100 \quad (1)$$

The selectivity was calculated using Eq. (2):

$$\%\ \text{selectivity} = \frac{\text{mass of product } i/M_i}{\text{mass of toluene reduced}/M_{\text{toluene}}} \times 100. \quad (2)$$

Synthesis of 5,10,15,20-tetraphenyl-21*H*,23*H*-porphine vanadium(IV) oxide (VOTPP)

Salicylic acid (3 g) and 5 cm^3 of benzaldehyde were mixed with 180 cm^3 of *o*-xylene and then heated and stirred to reflux. Then, a mixture of 2.8 cm^3 of pyrrole and 20 cm^3 of *o*-xylene was added slowly to the reaction system, refluxed for 4 h, and cooled to room temperature. Then, 30 cm^3 of absolute ethanol was added to the reaction system, and the mixture was allowed to stand overnight. The reaction mixture was filtered and washed thoroughly with hot distilled water and alcohol [11]. The filter cake was dried under vacuum for 5 h, and then dissolved ultrasonically in dichloromethane and filtered. The solution was set aside for crystallization at room temperature, yielding red–purple tetraphenylporphyrin (TPP).

Then, 6 cm^3 of phenol, 0.25 g of TPP, and 0.133 g of $VO(acac)_2$ were added to the flask and heated with stirring for 9 h [12]. After that, the mixture was cooled to room temperature, and a large amount of hot distilled water was added and filtered. The filter cake was washed thoroughly with methanol and dried under vacuum, and the pink–purple shiny crystal products (yield 93.4%) were recrystallized by slow evaporation of a CH_2Cl_2 solution. The synthetic route of VOTPP is shown in Scheme 1.

Oxidation of toluene

The aerobic oxidation of toluene was performed in a 250-cm^3 WHF-0.25 autoclave equipped with a gas inlet and vent, liquid sampler, safety rupture valve, piezometer, and thermowell. In a typical reaction, 100 cm^3 of toluene and 0.3 g of VOTPP were added into the reactor. The reactor was pressurized with oxygen to 0.8 MPa, and the reaction was initiated by agitating the reactor at 60 r/min when the temperature reached 145 °C. After the reaction was stopped, the mixture was cooled to room temperature and analyzed by HPLC and GC. The oxidation route of toluene is shown in Scheme 2.

References

1. Gizli A, Aytimur G, Alpay E, Atalay S (2008) Chem End Technol 31:409
2. Seper KW (2001) Chlorotoluenes, Benzyl Chloride, Benzal Chloride, and Benzotrichloride. In: Kirk-Othmer Encyclopedia of Chemical Technology, 5th edn, vol 6. John Wiley & Sons Inc, Hoboken, p 323
3. Li Y, Huang X, Li Y (2013) Sci Rep 3:1787
4. Partenheimer W (1995) Catal Today 23:69
5. Tang SW, Liang B (2007) Ind Eng Chem 46:7826
6. Parvulescu V, Constantin C, Su BL (2003) J Mol Catal A-Chem 202:171
7. Subrahmanyam C, Louis B, Viswanathan B, Renken A, Varadarajan TK (2005) Appl Catal A-Gen 282:67
8. Huang G, Wang PA, Liu SY, Guo YA, Zhou H, Zhao SK (2007) Catal Lett 114:174
9. Bastock TW, Clark JH, Martin K, Trenbirth BW (2002) Green Chem 4:615

10. Li YJ, Huang XQ, Li YJ, Xu YX, Wang Y, Zhu EB, Duan XF, Huang Y (2003) Sci Rep-UK 3:1787
11. Ul'yanova MI, Pervova MG, Slepukhin PA, Aksenova TV, Pestov AV (2018) Russ J Org Chem 54:687
12. Nie JF, Liu HC (2012) Pure Appl Chem 84:765
13. Mo M, Zheng M, Tang JS, Chen Y, Lu Q, Xun YY (2013) Res Chem Intermed 41:4067
14. Bottino A, Capannelli G, Comite A, Felice RD (2005) Catal Today 99:171
15. Bulushev DA, Kiwiminsker L, Renken A (2000) Catal Today 61:271
16. Huang G, Mo LQ, Cai JL, Cao X, Peng Y, Guo YA, Wei SJ (2015) Appl Catal B-Environ 162:364
17. Fang Z, Breslow R (2006) Org Lett 8:251
18. Qiu T, Xu XY, Qian XH (2009) J Chem Technol Biotechnol 84:1051
19. Deng W, Wan YP, Jiang H, Luo WP, Tan Z, Jiang Q, Guo CC (2014) Catal Lett 144:333
20. Adler AD, Longo FR, Finareii IJD (1967) J Org Chem 32:476
21. Tsutomu Y, Matteo A, Lorenzo T (2018) J Am Chem Soc 40:12090
22. Giovanna DL, Andrea R, Luigi MS (2007) Inorg Chem 46:5979
23. Biesaga M, Krystyna P, Trojanowicz M (2000) Talanta 51:209
24. Wang C, Tang W, Zhong H (2009) Chin J Chem 27:2020
25. Feng Y, Ong SL, Hu J (2003) Inorg Chem Commun 6:466
26. Ghanbari B, Shahhoseini L, Kubicki M (2017) Polyhedron 133:410
27. Peng C, Yao BH, Zhang W (2014) Chin J Chem Phys 27:200
28. Rahiman AK, Sreedaran S, Bharathi KS (2010) J Porous Mat 17:711
29. Hung W, Wei J (1980) Ind Eng Chem Process Des Dev 19:257
30. Gottfried JM, Flechtner K, Kretschmann A (2006) J Am Chem Soc 128:5644
31. Zang N, Dai F, Yan WW, Ruan WJ, Zhu ZA (2009) Chin J Inorg Chem 25:781
32. Li XK, He XH, Chen YW, Fan XL (2012) New Chem Mater 40:106
33. Zhou XT, Ji HB, Yuan QL (2008) J Porphyrins Phthalocyanines 12:94